LETTER

ACS chemical biology

A Derivatized Scorpion Toxin Reveals the Functional Output of Heteromeric KCNQ1–KCNE K^+ Channel Complexes

Trevor J. Morin and William R. Kobertz*

Department of Biochemistry and Molecular Pharmacology, Programs in Neuroscience and Chemical Biology, University of Massachusetts Medical School, 364 Plantation Street, Worcester, Massachusetts 01605-2324

ABSTRACT KCNE transmembrane peptides are a family of modulatory β-subunits that assemble with voltage-gated K^+ channels, producing the diversity of potassium currents needed for proper function in a variety of tissues. Although all five KCNE transcripts have been found in cardiac and other tissues, it is unclear whether two different KCNE peptides can assemble with the same K^+ channel to form a functional complex. Here, we describe the derivatization of a scorpion toxin that irreversibly inhibits KCNQ1 (Q1) K^+ channel complexes that contain a specific KCNE peptide. Using this KCNE sensor, we show that heteromeric complexes form, and the functional output from these complexes reveals a hierarchy in KCNE modulation of Q1 channels: KCNE3 > KCNE1 ≫ KCNE4. Furthermore, our results demonstrate that Q1/KCNE1/KCNE4 complexes also generate a slowly activating current that has been previously attributed to homomeric Q1/KCNE1 complexes, providing a potential functional role for KCNE4 peptides in the heart.

Cellular potassium efflux is controlled by the orchestrated openings and closings of K^+ channel proteins. To meet the potassium conduction requirements for a wide variety of tissues, K^+ channels co-assemble with different β-subunits to afford membrane-embedded complexes with distinctive gating properties. The KCNE type I transmembrane peptides are a class of β-subunits that assemble with and modulate the electrical output of voltage-gated K^+ channels (*1*). KCNE peptides are particularly fond of KCNQ1 (Q1) channels, as all five members (E1–E5) form complexes with this voltage-gated K^+ channel (*1*). The number of KCNE peptides in a K^+ channel complex is still debated. Studies have proposed two or four KCNE peptides per K^+ channel tetramer; however, alternative subunit compositions could not be ruled out (*2*–*4*). Q1 channels must assemble with KCNE peptides for proper physiological function, because mutations that disrupt complex formation give rise to congenital deafness and inherited cardiac arrhythmias (*5, 6*). In the heart, the Q1/E1 K^+ channel complex has long been thought to generate the slowly activating cardiac I_{Ks} current (*7, 8*). In contrast, E2 and E3 subunits have been shown to assemble with Q1 channel subunits in epithelial cells where they maintain salt and water homeostasis (*9, 10*). The biological roles of Q1/E4 and Q1/E5 complexes have yet to be defined.

Because the functional output of Q1 channels is controlled by KCNE peptides, their tissue distribution has been assumed to underlie Q1–KCNE complex function *in vivo*. Recently, all five KCNE transcripts have been detected in cardiac (*11, 12*) and other tissues (*13*), raising the possibility that two different KCNE peptides can assemble with the same Q1 channel to form a heteromeric complex. Determining the functional output of heteromeric Q1–KCNE complexes has been hampered by the fact that macroscopic electrical recordings measure the total current from a cell, making it difficult to deconvolute the contribution of heteromeric complexes (*e.g.*, Q1/E1/E4) from two populations of homomeric complexes (*e.g.*, Q1/E1 and Q1/E4) functioning at the cell surface. Co-immunoprecipitation of one KCNE peptide by another KCNE peptide has indirectly hinted at heteromeric complex formation (*14*). However, these qualitative biochemical experiments are unsatisfying given that it is unclear whether these precipitated complexes are functional. Therefore, we utilized a tethered blocker approach in combination with electrophysiological recordings to determine the KCNE composition and functional consequences of heteromeric Q1–KCNE K^+ channel complex formation.

KCNE peptides have a striking effect on the opening and closing of Q1 channels, and these gating differences have been traditionally used to identify the composition of homomeric Q1–KCNE complexes

*Corresponding author, william.kobertz@umassmed.edu.

Received for review April 18, 2007 and accepted May 31, 2007.

Published online June 29, 2007

10.1021/cb700089s CCC: $37.00

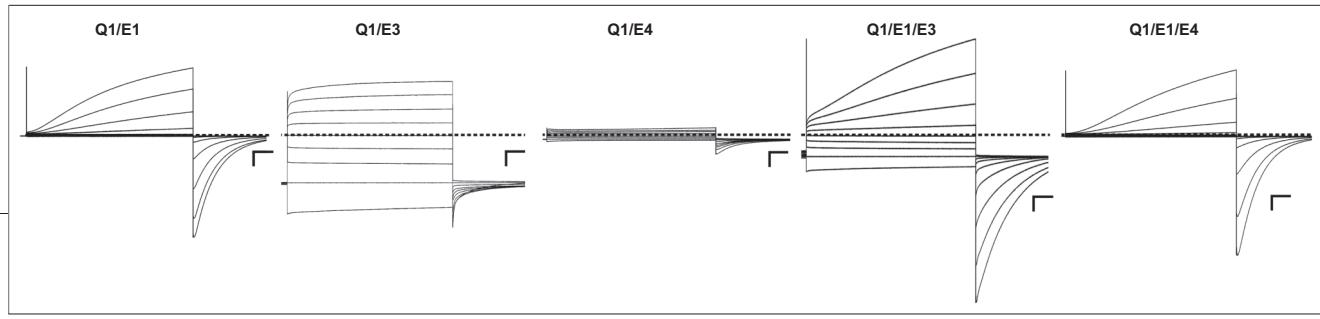

Figure 1. Coexpression of Q1 channels with two different KCNE peptides gives rise to an amalgam of voltage-dependent and -independent currents. Two-electrode voltage clamp recordings for homo- and heteromeric Q1–KCNE complexes. Currents were elicited by a family of command voltages from −100 to 60 mV at 20-mV increments and recorded in KD50 solution. Dashed line indicates zero current. Scale bars represent 1 μA and 0.5 s.

(Figure 1). Q1/E1 complexes are strongly voltage-dependent and upon depolarization give rise to a slowly activating K^+ current (*7, 8*), whereas Q1/E3 complexes are open at both negative and positive voltages and have nearly instantaneous gating kinetics (Figure 1) (*10*). In contrast, when Q1 assembles with E4, the complexes are essentially nonconducting at the plasma membrane (Figure 1) (*15*). Coexpression of Q1 and E1 with E3 or E4 results in an amalgam of currents (Figure 1), and visual inspection or activation curve analysis (Supplementary Figure 1) does not reveal whether there are heteromeric Q1–KCNE complexes functioning at the plasma membrane. To detect KCNE peptides in functioning Q1 channel complexes, we synthetically modified charybdotoxin (CTX) to specifically react with cysteine residues within the N-termini of KCNE peptides (Figure 2, panel a). CTX is a peptide scorpion toxin that reversibly binds K^+ channels with high affinity (*16, 17*). Previous studies with CTX have shown that an arginine on the backside of the toxin can be mutated to cysteine for derivatization without affecting its affinity for K^+ channels (*18, 19*). To convert CTX into a cysteine-reactive inhibitor (CTX-Mal), the mixed disulfide protected R19C CTX mutant was treated with DTT followed by the addition of 100-fold molar excess bis-maleimide (Methods section).

Because CTX does not inhibit native Q1/E1 complexes, we utilized a variant of Q1 that is blocked by nanomolar concentrations of toxin (*2*). CTX-sensitive Q1/E1 complexes do not possess any extracellular cysteines and thus CTX-Mal should reversibly bind to these complexes. When cells expressing CTX-sensitive Q1/E1 complexes were treated with 10 nM CTX-Mal, the current was blocked, and then upon washout, it fully recovered to pretreated levels, demonstrating that inhibition was reversible (Figure 2, panel b). Q1/E3 complexes were also reversibly blocked by CTX-Mal when the lone cysteine in E3 (C31S) was removed by mutagenesis (Figure 2, panel b, second graph). These control experiments showed that chemical derivatization of CTX did not disrupt binding to the Q1 channel pore. We next cysteine-scanned the N-terminus of E1 to find residues that were covalently modifiable by CTX-Mal. The N-termini of KCNE peptides are ideal for cysteine mutagenesis because these regions in E1 and E3 are not required for assembly with or modulation of Q1 channels (*20, 21*). Mutation of three E1 residues (Thr14, Gln22, and Ser34) to cysteine resulted in Q1/E1 complexes with wild-type gating kinetics that were irreversibly blocked by CTX-Mal. Q1/$E1_{T14C}$ complexes were the most reactive, showing no relief of inhibition upon washout of CTX-Mal (Figure 2, panel b, third graph). Covalent tethering of CTX-Mal to Q1/$E1_{T14C}$ required binding to the channel pore given that the reaction was completely prevented by competitive inhibition with 250 nM CTX (Figure 2, panel b, fourth graph). In all experiments, only ~85% of the total current could be inhibited (reversibly or irreversibly); even in the presence of 250 nM wild-type CTX, which based on the calculated dissociation constant for CTX-sensitive Q1/E1 complexes should afford >99.9% inhibition (*2*). We did not expect 100% block because *Xenopus* oocytes possess low levels of endogenous, CTX-insensitive Q1 channels that migrate to the cell surface with the injection of KCNE mRNAs (Supplementary Figure 2) (*2, 7*).

Armed with a reagent to detect KCNE peptides in K^+ channel complexes, we determined whether Q1/E1/E3 complexes assemble and are functional. We first placed

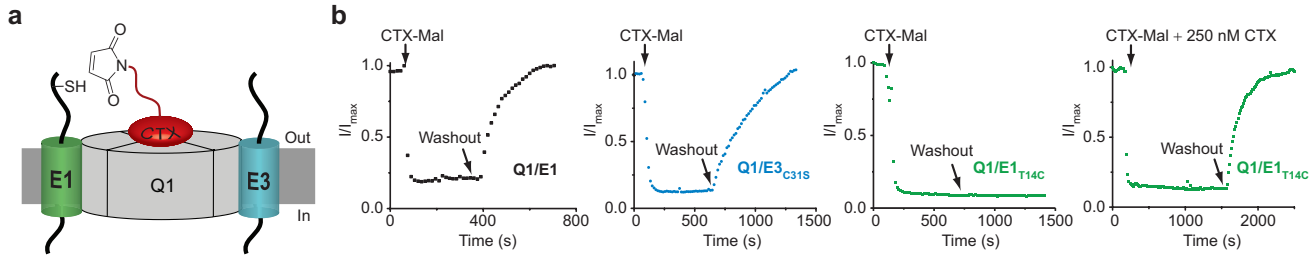

Figure 2. Strategy and utilization of CTX-Mal for identifying KCNE peptides in functioning Q1–KCNE complexes. a) Cartoon depiction of the toxin tethering reaction between CTX-Mal and a cysteine residue in E1. b) Inhibition of Q1–KCNE complexes with (10 nM) CTX-Mal in ND96 solution. Current was monitored at 20 mV every 15 s. Q1/E1 and Q1/$E3_{C31S}$ complexes lack extracellular cysteine residues. Single cysteine containing Q1/$E1_{T14C}$ complexes were irreversibly inhibited by CTX-Mal after washout; inhibition was completely prevented in the presence of excess (250 nM) CTX.

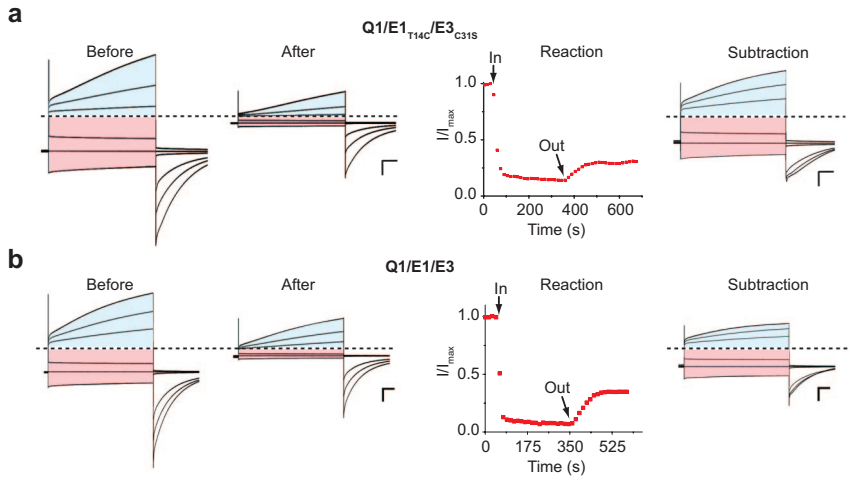

Figure 3. Detection of heteromeric Q1/E1/E3 complexes with CTX-Mal: a) Q1/E1$_{T14C}$/E3$_{C31S}$. b) Q1/E1/E3 (using native cysteine (C31) in E3). Current traces shown are pretreatment (Before) and after washout (After) of 10 nM CTX-Mal. Currents were measured in KD50 solution and were from command voltages (−100, −80, −60, 0, 20, and 40 mV). Subtraction traces are a mathematical difference of the After and Before traces. Outward currents are shaded blue; inward are shaded pink. Dashed line indicates zero current. Scale bars represent 1 μA and 0.5 s. Reaction profiles (Reaction) with 10 nM CTX-Mal were monitored at −100 mV every 15 s in KD50 solution. For Q1/E1$_{T14C}$/E3$_{C31S}$, 78% ± 2% of the CTX-sensitive current was irreversibly inhibited after washout and for Q1/E1/E3 74% ± 4%. Data were averaged from three to five oocytes ± SEM.

the target cysteine in E1. Coexpression of Q1/E1$_{T14C}$/E3$_{C31S}$ resulted in both outward and inward currents in response to a family of depolarizations in 50 mM external K^+ (Figure 3, panel a, Before). This external solution (KD50) allows for the visualization of the inward currents (shaded pink); however, this concentration of external K^+ noticeably slows the activation/deactivation kinetics of some Q1–KCNE complexes (Figures 1 and 3) compared with ND96 (2 mM KCl) solution (Figure 4). Treatment of these cells with CTX-Mal covalently modifies and irreversibly blocks Q1 channel complexes that have assembled with E1$_{T14C}$ peptides. Upon washout, ~80% of the CTX-sensitive current generated by a −100 mV test potential was irreversibly inhibited (Figure 3, panel a, Reaction). Examination of the current–voltage traces after CTX-Mal washout (Figure 3, panel a, After) shows a mixture of E1 and E3 modulated Q1 currents. Because CTX-Mal irreversibly blocks all of the CTX-sensitive current in exogenously expressed Q1/E1$_{T14C}$ complexes (Figure 2, panel c, third graph), we postulate that the remaining Q1/E1 current is due to endogenous (CTX-insensitive) Q1 channels that have assembled with E1$_{T14C}$ peptides (Supplementary Figure 2). To visualize the currents irreversibly blocked by CTX-Mal, we mathematically subtracted the remaining current after block from the before block currents. The subtracted traces are a mixture of currents from Q1/E1 homomers and Q1/E1/E3 heteromers. However, because homomeric Q1/E1 complexes are closed and nonconducting with test potentials <-30 mV (Figure 1), the inward currents in the subtracted traces (Figure 3, panel a) are entirely from Q1/E1$_{T14C}$/E3$_{C31S}$ complexes. Unlike the inward currents, the outward currents (shaded blue) in the subtracted traces are contaminated with slowly activating homomeric Q1/E1$_{T14C}$ currents. To determine whether Q1/E1/E3 complexes possess any time-dependent activation at positive potentials, we utilized the native cysteine in E3 and looked at irreversible block of outward currents in wild-type Q1/E1/E3 complexes. The blocked outward currents in this configuration will still be a mixture of homo- and heteromeric complexes; however, the homomeric complexes are Q1/E3, which are devoid of slow gating (Figure 1). Thus, any slow gating observed would be due to heteromeric Q1/E1/E3 complexes. CTX-Mal treatment and subsequent washout of cells expressing Q1/E1/E3 resulted in a reduction of both inward and outward currents as before (Figure 3, panel b). Mathematical subtraction reveals that heteromeric Q1/E1/E3 complexes slowly activate at positive voltages and slowly deactivate upon repolarization (Figure 3, panel b, Subtraction). In total, these results show that the Q1/E1/E3 complex generates current with the combined properties of homomeric Q1/E1 and Q1/E3 complexes: it is a heteromeric complex that is open at negative potentials but slowly activates with positive depolarizations.

We next examined whether Q1/E1/E4 complexes were functional. E4 is the most abundant KCNE transcript in heart (*11, 12*), yet when the peptide assembles with Q1, it produces a nonconducting channel complex (Figure 1) (*15*). Therefore, to detect functional Q1/E1/E4 complexes, the cysteine residue was placed in E4. When E4$_{L2C}$ was coexpressed with Q1/E1, the resultant CTX-sensitive currents in ND96 solution were irreversibly blocked (52% ± 3%) by CTX-Mal upon washout (Figure 4, panel a). Irreversible blockade of any current indicates Q1/E1/E4 complex assembly given that homomeric Q1/E4$_{L2C}$ complexes are like wild-type Q1/E4 and nonconducting (data not shown). The amount of irreversible inhibition measured was predictably dependent on the ratio of E1/E4$_{L2C}$ expressed. Injection ratios that favored the formation of Q1/E1

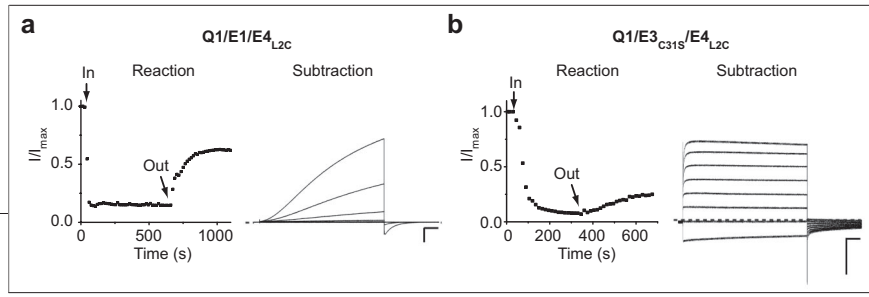

Figure 4. KCNE4 peptides form heteromeric complexes with Q1 and KCNE1 or KCNE3. a) Q1/E1/$E4_{L2C}$. b) Q1/$E3_{C31S}$/$E4_{L2C}$. Reaction profiles (Reaction) with 10 nM CTX-Mal were monitored at 20 mV every 15 s in ND96 solution. For Q1/E1/$E4_{L2C}$, 52% ± 3% of the CTX-sensitive current was irreversibly inhibited after washout and for Q1/E3/$E4_{L2C}$ 80% ± 1%. Data were averaged from two to five oocytes ± SEM. Families of currents (Subtraction) in ND96 were generated by subtracting the pretreated currents from the currents elicited after washout of CTX-Mal. The Before and After currents for panels a and b are shown in Supplementary Figure 3. Command voltages were from −100 to 40 mV with 20 mV steps. Dashed line indicates zero current. Scale bars represent 1 μA and 0.5 s.

homomers resulted in a reduction of irreversible block, whereas injection of more $E4_{L2C}$ mRNA resulted in an increase of irreversible block (Supplementary Figure 4). Subtraction of the after traces from the before traces (Supplementary Figure 3) revealed the gating kinetics of Q1/E1/E4 complexes (Figure 4, panel a, Subtraction), which resemble the cardiac I_{Ks} current that has been attributed to Q1/E1 complexes. E4 also forms functional heteromeric Q1 complexes with E3. Q1/$E3_{C31S}$/$E4_{L2C}$ complexes were irreversibly blocked by CTX-Mal in ND96 solution (Figure 4, panel b). Although E4 is present in both heteromeric complexes studied, the peptide has little effect on the gating kinetics. Thus for Q1 channels, E3 and E1 dictate gating in heteromeric complexes with E4 peptides.

Our results using CTX-Mal demonstrate that a tetrameric Q1 channel can simultaneously assemble with two different KCNE peptides. Although we show that heteromeric Q1–KCNE complexes form, we cannot determine the assembly preference for KCNE peptides with Q1 subunits because we are looking at an endpoint (current expression) and not the biogenesis and stability of the protein subunits. The formation of heteromeric complexes requires that there are at least two KCNE peptides in the K^+ channel complex; however, irreversible inhibition with CTX-Mal cannot distinguish between two or more peptides within the complex, which is still a surprisingly unsettled issue (*2–4*). Our results also indicate that the N-termini of KCNE peptides are near the Q1 channel outer vestibule since the linker connecting CTX to the maleimide is too short to reach beyond the S3–S4 loop of the voltage sensor (*22*). On the basis of a recent NMR structure of CTX bound to a bacterial K^+ channel (*23*), we tentatively position the KCNE N-terminus within ~20 Å of the ion conduction pathway. CTX-Mal enabled us to determine that certain KCNE peptides govern Q1 modulation in heteromeric complexes: E3 > E1 ≫ E4, where the dominant peptide has substantial control over the opening and closing of the channel. This hierarchy of KCNE modulation of Q1 channels has several implications on KCNE physiology. In the heart, it has been assumed that homomeric Q1/E1 complexes produce the unmistakably slowly activating/deactivating current involved in repolarization (*7, 8*). E4 may also generate the cardiac I_{Ks} current because Q1/E1/E4 and Q1/E1 complexes have similar gating kinetics. Likewise, in most epithelial cells where the resting membrane potential is negative, the assembly of E1, E4, or E5 with Q1 has been questioned given that these complexes would be essentially closed. However, E1 and E4 peptides can act as structural surrogates in Q1/E3 heteromeric complexes to produce channels that are open at negative potentials and thus may partake in salt and water homeostasis. In either case, these heteromeric complexes can substitute for homomeric complexes; however, they require the presence of the dominant KCNE peptide, consistent with KCNE knockout mice studies (*9, 24*). In contrast, overexpression of constitutively conducting Q1/E1/E3 complexes could be detrimental in maintaining the cardiac action and resting potentials, suggesting that cells regulate Q1–KCNE assembly. Simple binary transcriptional regulation of functionally opposed KCNE peptides could be used to control the potassium efflux of a cell. Alternatively, KCNE assembly with Q1 channel subunits may be regulated at the protein folding level. If Q1–KCNE assembly is chaperone-mediated, these proteins must reside in either the ER or cis-Golgi since KCNE peptides assemble with Q1 channels early in the secretory pathway (*25*).

We have used a synthetically modified scorpion toxin to detect Q1 subunit assembly with a mixed KCNE population. CTX-Mal can also be used to disentangle the phenotypic effects of KCNE mutations on assembly from those on modulation by deconvolving the functional contributions of unpartnered Q1 channels and mutant Q1–KCNE complexes. The discovery that heteromeric Q1–KCNE complexes form implies that other voltage-gated K^+ channels will be amenable to coassembly with two different KCNE peptides. Given the cadre of scorpion and spider toxins available to specifically inhibit a wide range of ion channels, our approach can be readily applied to study other membrane-embedded β-subunits in functioning ion channel complexes.

METHODS

Mutagenesis and *in Vitro* Transcription. The CTX sensitive Q1 construct (*2*), E1, E3, and E4 were subcloned into a vector containing the 5′ and 3′ untranslated regions from the *Xenopus* β-globin gene for optimal expression in *Xenopus* oocytes. Single point mutations in KCNE peptides were introduced using QuikChange site-directed mutagenesis (Stratagene) and confirmed by DNA sequencing of the entire gene. E1 and E3 constructs possessed the hemagglutinin A tag, YPYDVPDYA, in the N-terminus between residues 22 and 23 and 11 and 12, respectively, which has been shown to increase toxin affinity (*2*). The complementary DNA plasmids were linearized, and complementary RNA was synthesized by run-off transcription using SP6 or T7 RNA polymerase (Promega).

Electrophysiology. Standard techniques were used for preparation of and recording from *Xenopus* oocytes by two-electrode voltage clamp 2–4 d (5–6 d for E4) after cRNA injection (*26*). Oocytes expressing KCNE extracellular cysteine residues were stored in ND96 bathing solution (96 mM

acs chemical biology

NaCl, 2 mM KCl, 1.8 mM $CaCl_2$, 5 mM HEPES, pH 7.4, 50 μg mL^{-1} gentamicin containing 1 mM L-glutathione (Sigma)) and incubated in ND96 recording (96 mM NaCl, 2 mM KCl, 0.3 mM $CaCl_2$, 1 mM $MgCl_2$, 5 mM HEPES, pH 7.4, containing 1 mM TCEP (CalBioChem)) for 10 min prior to recording. cRNA injection ratios were as follows: Q1/E1, Q1/$E1_{T14C}$, Q1/E3, Q1/$E3_{C31S}$, and Q1/$E4_{L2C}$, 3:1; Q1/$E1_{T14C}$/$E3_{C31S}$, Q1/E1/E3, and Q1/$E4_{L2C}$/$E3_{C31S}$, 4:1:0.2; Q1/E1/$E4_{L2C}$, 4:1:1. Current–voltage relationships were measured in ND96 or KD50 (50 mM KCl, 48 mM NaCl, 0.3 mM $CaCl_2$, 1 mM $MgCl_2$, 5 mM HEPES, pH 7.4) by holding at −80 mV and pulsing for 2 or 4 s to potentials between −100 and +60 mV in 10-mV increments. Activation curves were generated from tail currents and measured 6 ms after repolarization to −80 mV in KD50, as was previously described for channels with basal activation (*21*). For CTX experiments, bath solutions also contained 50 μg mL^{-1} bovine serum albumin. Solution exchanges were performed by gravity-fed perfusion system with a chamber clearing time of ~10 s. Families of currents before and after block were recorded in the appropriate bath solution by holding at −80 mV and pulsing from −100 to 60 mV in 20 mV increments. Currents from heteromeric Q1–KCNE complexes were revealed by subtracting postblock family traces from preblock families (Clampfit 9.0 Axon Instruments).

CTX Derivatization. Recombinant CTX R19C was purified and the protected CTX-MTSET adduct was prepared according to Shimony *et al.* (*18*). CTX-Mal was synthesized as follows: 16 nmol of CTX-MTSET in 2 mL of Buffer C (10 mM NaCl, 10 mM KPi, pH 7.4) was reduced with 1 mM DTT for 30 min and bound to a SP Sephedex (Sigma) cation exchange column. DTT was washed from the column using 150 mL of Buffer C, and the resin bound CTX was labeled with 3 mL of 5 mM $BM[PEO]_3$ (Pierce) in Buffer C. After 10 min, the column was washed with Buffer C to remove excess label, and CTX-Mal was eluted with 1 M NaCl in 10 mM KPi, pH 7.4. CTX-Mal was desalted and HPLC purified using a C18 column (4.6 mm × 250 mm) eluting with solvent A (0.1% TFA)/solvent B (acetonitrile) gradient 10% to 40% B over 30 min. The concentration of purified CTX-Mal was determined by UV spectrometry (OD_{280} of 1.0 = 100 μM CTX (*18*)) and labeling efficiency of CTX-R19C was determined to be 35% ± 5% (n = 10). The purified product was confirmed by electrospray ionization mass spectrometry (see Supporting Information) and was aliquoted, lyophilized, and stored at −20 °C. Individual aliquots were resuspended in recording solutions immediately prior to use.

Acknowledgment: We thank A. George (Vanderbilt University) for the E4 clone. W. Kobertz was supported in part by a Burroughs-Wellcome Foundation for a Career Award in the Biomedical Sciences. This work was supported by the National Institutes of Health Grants GM0707650 and DC007669.

Supporting Information Available: This material is free of charge *via* the Internet.

REFERENCES

1. McCrossan, Z. A., and Abbott, G. W. (2004) The MinK-related peptides, *Neuropharmacology 47*, 787–821.
2. Chen, H., Kim, L. A., Rajan, S., Xu, S., and Goldstein, S. A. (2003) Charybdotoxin binding in the I_{Ks} pore demonstrates two MinK subunits in each channel complex, *Neuron 40*, 15–23.
3. Wang, W., Xia, J., and Kass, R. S. (1998) MinK-KvLQT1 fusion proteins, evidence for multiple stoichiometries of the assembled I_{sK} channel, *J. Biol. Chem. 273*, 34069–34074.
4. Wang, K. W., and Goldstein, S. A. (1995) Subunit composition of minK potassium channels, *Neuron 14*, 1303–1309.
5. Splawski, I., Shen, J., Timothy, K. W., Lehmann, M. H., Priori, S., Robinson, J. L., Moss, A. J., Schwartz, P. J., Towbin, J. A., Vincent, G. M., and Keating, M. T. (2000) Spectrum of mutations in long-QT syndrome genes. KVLQT1, HERG, SCN5A, KCNE1, and KCNE2, *Circulation 102*, 1178–1185.
6. Tyson, J., Tranebjaerg, L., McEntagart, M., Larsen, L. A., Christiansen, M., Whiteford, M. L., Bathen, J., Aslaksen, B., Sorland, S. J., Lund, O., Pembrey, M. E., Malcolm, S., and Bitner-Glindzicz, M. (2000) Mutational spectrum in the cardioauditory syndrome of Jervell and Lange-Nielsen, *Hum. Genet. 107*, 499–503.
7. Sanguinetti, M. C., Curran, M. E., Zou, A., Shen, J., Spector, P. S., Atkinson, D. L., and Keating, M. T. (1996) Coassembly of K_VLQT1 and minK (IsK) proteins to form cardiac I_{Ks} potassium channel, *Nature 384*, 80–83.
8. Barhanin, J., Lesage, F., Guillemare, E., Fink, M., Lazdunski, M., and Romey, G. (1996) K_VLQT1 and IsK (minK) proteins associate to form the I_{Ks} cardiac potassium current, *Nature 384*, 78–80.
9. Roepke, T. K., Anantharam, A., Kirchhoff, P., Busque, S. M., Young, J. B., Geibel, J. P., Lerner, D. J., and Abbott, G. W. (2006) The KCNE2 potassium channel ancillary subunit is essential for gastric acid secretion, *J. Biol. Chem. 281*, 23740–23747.
10. Schroeder, B. C., Waldegger, S., Fehr, S., Bleich, M., Warth, R., Greger, R., and Jentsch, T. J. (2000) A constitutively open potassium channel formed by KCNQ1 and KCNE3, *Nature 403*, 196–199.
11. Lundquist, A. L., Manderfield, L. J., Vanoye, C. G., Rogers, C. S., Donahue, B. S., Chang, P. A., Drinkwater, D. C., Murray, K. T., and George, A. L., Jr (2005) Expression of multiple KCNE genes in human heart may enable variable modulation of I_{Ks}, *J. Mol. Cell. Cardiol. 38*, 277–287.
12. Bendahhou, S., Marionneau, C., Haurogne, K., Larroque, M. M., Derand, R., Szuts, V., Escande, D., Demolombe, S., and Barhanin, J. (2005) *In vitro* molecular interactions and distribution of KCNE family with KCNQ1 in the human heart, *Cardiovasc. Res. 67*, 529–538.
13. Lundquist, A. L., Turner, C. L., Ballester, L. Y., and George, A. L., Jr (2006) Expression and transcriptional control of human KCNE genes, *Genomics 87*, 119–128.
14. Wu, D. M., Jiang, M., Zhang, M., Liu, X. S., Korolkova, Y. V., and Tseng, G. N. (2006) KCNE2 is colocalized with KCNQ1 and KCNE1 in cardiac myocytes and may function as a negative modulator of I_{Ks} current amplitude in the heart, *Heart Rhythm 3*, 1469–1480.
15. Grunnet, M., Jespersen, T., Rasmussen, H. B., Ljungstrom, T., Jorgensen, N. K., Olesen, S. P., and Klaerke, D. A. (2002) KCNE4 is an inhibitory subunit to the KCNQ1 channel, *J. Physiol. 542*, 119–130.
16. Smith, C., Phillips, M., and Miller, C. (1986) Purification of charybdotoxin, a specific inhibitor of the high-conductance Ca^{2+}-activated K^+ channel, *J. Biol. Chem. 261*, 14607–14613.
17. Goldstein, S. A., Pheasant, D. J., and Miller, C. (1994) The charybdotoxin receptor of a Shaker K^+ channel: peptide and channel residues mediating molecular recognition, *Neuron 12*, 1377–1388.
18. Shimony, E., Sun, T., Kolmakova-Partensky, L., and Miller, C. (1994) Engineering a uniquely reactive thiol into a cysteine-rich peptide, *Protein Eng. 7*, 503–507.
19. Posson, D. J., Ge, P., Miller, C., Bezanilla, F., and Selvin, P. R. (2005) Small vertical movement of a K^+ channel voltage sensor measured with luminescence energy transfer, *Nature 436*, 848–851.
20. Takumi, T., Moriyoshi, K., Aramori, I., Ishii, T., Oiki, S., Okada, Y., Ohkubo, H., and Nakanishi, S. (1991) Alteration of channel activities and gating by mutations of slow I_{sK} potassium channel, *J. Biol. Chem. 266*, 22192–22198.
21. Gage, S. D., and Kobertz, W. R. (2004) KCNE3 truncation mutants reveal a bipartite modulation of KCNQ1 K^+ channels, *J. Gen. Physiol. 124*, 759–771.
22. Blaustein, R. O., Cole, P. A., Williams, C., and Miller, C. (2000) Tethered blockers as molecular 'tape measures' for a voltage-gated K^+ channel, *Nat. Struct. Biol. 7*, 309–311.
23. Yu, L., Sun, C., Song, D., Shen, J., Xu, N., Gunasekera, A., Hajduk, P. J., and Olejniczak, E. T. (2005) Nuclear magnetic resonance structural studies of a potassium channel-charybdotoxin complex, *Biochemistry 44*, 15834–15841.
24. Vetter, D. E., Mann, J. R., Wangemann, P., Liu, J., McLaughlin, K. J., Lesage, F., Marcus, D. C., Lazdunski, M., Heinemann, S. F., and Barhanin, J. (1996) Inner ear defects induced by null mutation of the isk gene, *Neuron 17*, 1251–1264.
25. Chandrasekhar, K. D., Bas, T., and Kobertz, W. R. (2006) KCNE1 subunits require co-assembly with K^+ channels for efficient trafficking and cell surface expression, *J. Biol. Chem. 281*, 40015–40023.
26. Rudy, B., and Iverson, L. E. (1992) Ion Channels, *Methods Enzymol. 207*, 225–345.